



Analysis of elastic–plastic problems using edge-based smoothed finite element method

X.Y. Cui^{a,b}, G.R. Liu^{b,c}, G.Y. Li^{a,*}, G.Y. Zhang^c, G.Y. Sun^a

^a State Key Laboratory of Advanced Design and Manufacturing for Vehicle Body, Hunan University, Changsha 410082, PR China

^b Centre for Advanced Computations in Engineering Science (ACES), Department of Mechanical Engineering, National University of Singapore, 9 Engineering Drive 1, 117576 Singapore, Singapore

^c Singapore-MIT Alliance (SMA), E4-04-10, 4 Engineering Drive 3, 117576 Singapore, Singapore

ARTICLE INFO

Article history:

Received 5 October 2008

Received in revised form

8 December 2008

Accepted 10 December 2008

Keywords:

Numerical methods

Meshfree methods

Elastic–plastic analysis

FEM

ES-FEM

ABSTRACT

In this paper, an edge-based smoothed finite element method (ES-FEM) is formulated for stress field determination of elastic–plastic problems using triangular meshes, in which smoothing domains associated with the edges of the triangles are used for smoothing operations to improve the accuracy and the convergence rate of the method. The smoothed Galerkin weak form is adopted to obtain the discretized system equations, and the numerical integration becomes a simple summation over the edge-based smoothing domains. The pseudo-elastic method is employed for the determination of stress field and Hencky's total deformation theory is used to define effective elastic material parameters, which are treated as field variables and considered as functions of the final state of stress fields. The effective elastic material parameters are then obtained in an iterative manner based on the strain controlled projection method from the uniaxial material curve. Some numerical examples are investigated and excellent results have been obtained demonstrating the effectivity of the present method.

© 2008 Published by Elsevier Ltd.

1. Introduction

For the analysis and design in engineering structures, the elasto-plastic behavior of structure materials needs often to be considered. However, the complicated nonlinear stress–strain relationship and the loading path dependency in the plastic range make the analysis tedious. In the past several decades, the finite element method has been well developed and used as an important tool to analyze material nonlinear problems in practical engineering applications [1–4]. However, the displacement-based fully compatible finite element method has an inherent characteristic known as the overly-stiff phenomenon, especially when linear triangular elements are used.

To overcome the overly-stiff phenomenon and effectively “soften” the discretized system, Liu et al. have applied the smoothing technique [5] in a number of meshing free and finite element settings. A generalized gradient smoothing technique [6] has been proposed and used to establish weakened weak (W^2) formulations known as the generalized smoothed Galerkin weak form [7] that allows the use of discontinuous shape functions. Some

important properties including variational consistence, convergence, upper bound and soft effects of W^2 models have been revealed, proved or examined in detail. Liu et al. have also suggested various ways (cell-based, node-based, and edge-based) to create the smoothing domains for models of desired properties. In models using finite elements, cell-based smoothing domains are created by further dividing the elements into one or more smoothing cells (SC), leading to the so-called smoothed finite element method (SFEM) [8–10]. As SFEM computes the integrals along the edge of the smoothing domains, no derivatives of shape functions are needed, no mapping is required, and simple point interpolation methods can be used. It works well for very heavily distorted mesh, in addition to a number of important properties, such as the softening effects, better accuracy and upper bound for some class of problems. Using the node-based smoothing operation, NS-FEM was also been formulated that can often provide upper bound solutions for force driven problems [11]. Using the point interpolation method for shape function construction, a node-based smoothed point interpolation method (NS-PIM or LC-PIM) was formulated [12,13] and extended for heat transfer and thermoelasticity problems [14]. Liu and Zhang [13] proved that the NS-PIM is variationally consistent, can provide much better stress results, and more importantly can often provide upper bound solution in energy norm (for force driven problems). It is found,

* Corresponding author. Tel.: +86 731 8821717; fax: +86 731 8822051.

E-mail address: gyli@hnu.cn (G.Y. Li).

however, the NS-FEM or NS-PIM is too soft and hence has spurious modes when used for dynamic problems. Recently, an edge-based smoothed finite element method (ES-FEM) [15] has been proposed for 2D solid mechanics problems using edge-based smoothing domains. It has been found that the ES-FEM model is of closed-to-exact stiffness and gives ultra-accurate (one order more accurate) solution when triangular elements are used compared with the FEM.

A number of numerical techniques has been developed so far to solve the elasto-plasticity problems. The idea of using elastic solutions for approximation of inelastic behavior has been receiving much interest. Neuber [16] obtained elasto-plastic stress and strains at the stress concentration point using elastic solutions in early 1960s. Dhalla and Jones [17] used finite element elastic analysis for approximation of limit loads for pressure vessels and piping design. Based on this method, Seshadri [18] developed a generalized local stress and strain (GLOSS) method and used it to approximate plastic strains at local regions. Jahed et al. [19] developed a comprehensive method for solving pressure vessel problems in the elasto-plastic range based on elastic solutions. Babu and Iyer [20] developed a robust method using relaxation method, based on the GLOSS method, and an attempt was made to satisfy force equilibrium in the plastic range. Chen and Ponter performed shakedown and limit analyses for 3-D structures [21] and integrity assessment for a tubeplate [22] using linear matching method. This method also applied to the high temperature life integrity of structures [23,24]. Recently, Desikan and Sethuraman [25] proposed a pseudo-elastic finite element method for the determination of inelastic material parameters. In this method, material nonlinear problem was solved using the pseudo-elastic linear finite element method with suitable updation of elastic material properties during the process of iteration. Some researchers have adopted this method to solve material nonlinear problems, such as Sethuraman and Reddy [26], Dai et al. [27] and Gu et al. [28].

In this paper, the edge-based smoothed finite element method (ES-FEM) is formulated for solving material nonlinear problems based on Hencky's deformation theory. The problem domain is first discretized into a set of triangular elements and the smoothing domains associated with the edges of the triangles are then further formed. The material parameters are considered as field variables, and the linear elastic ES-FEM analysis will be carried out to get the pseudo-stress distributions. The stresses in each edge smoothing domain are constants, and the stresses at the nodes will be obtained by averaging the values of the associated smoothing domains. An iteration procedure is used to update the material parameters until equivalent stress-strain point in all smoothing domains coincide with the uniaxial experimental material curve. The strain controlled projection method is employed to calculate these effective material parameters. Problems with three material models, elastic-perfectly plastic material, work-hardening material and Ramberg-Osgood model, are presented to illustrate the effectivity of the ES-FEM formulation for the elasto-plastic analysis through comparing the numerical results with those obtained by the finite element commercial software ABAQUS.

2. ES-FEM formulations

As shown in Fig. 1, the problem domain Ω is divided into N_{element} triangular elements with a total of N_{edge} edges. Based on the triangular elements, smoothing domain for each edge is formed by sequentially connecting two end points of the edge and centroids of its surrounding triangles, such that $\Omega = \Omega_1 \cup \Omega_2 \cup \dots \cup \Omega_{N_{\text{edge}}}$ and $\Omega_i \cap \Omega_j = \emptyset$ ($i \neq j, i = 1, \dots, N_{\text{edge}}, j = 1, \dots, N_{\text{edge}}$). In the ES-FEM, the displacement interpolation is element based as in the FEM, but the integration is based on the smoothing domains that are used for strain filed smoothing.

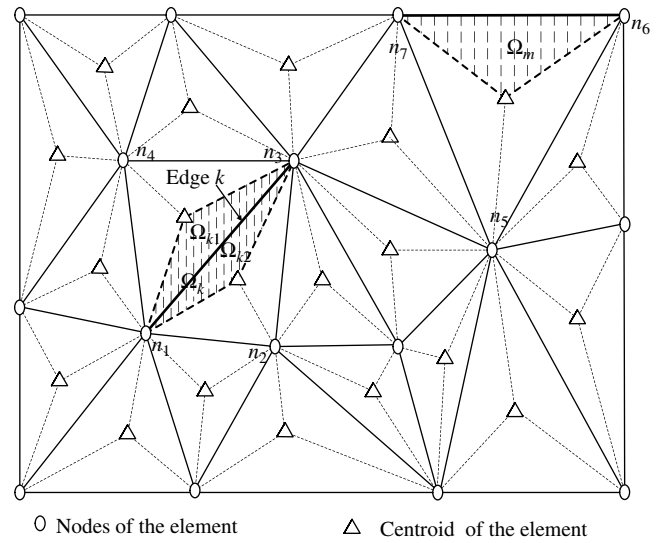


Fig. 1. The problem domain is divided into N_{element} triangular elements with a total of N_{edge} edges. Interior edge k is sandwiched in the smoothing domain Ω_k . Smoothing domain Ω_m for the boundary edge m is a triangle. There are N_k nodes that influence the k th smoothing domain Ω_k . For domains associated with boundary edges $N_k = 3$; for example, nodes n_5, n_6 and n_7 influence Ω_m . For domains associated with interior edges $N_k = 4$; for example, nodes n_1, n_2, n_3 and n_4 influence Ω_k .

At any point in a triangular element, the displacement field \mathbf{u} in the element is interpolated using the nodal displacements at the nodes of the element by the linear shape functions, same as in the standard linear FEM,

$$\mathbf{u}(\mathbf{x}) = \sum_{i=1}^3 \mathbf{N}_i(\mathbf{x}) \mathbf{d}_i \tag{1}$$

where $\mathbf{d}_i = \{u_i, v_i\}^T$ is the nodal displacement at node i , $\mathbf{N}_i(\mathbf{x})$ is a diagonal matrix of shape functions.

Using strain-displacement equations, the compatible strain in each element can be given by

$$\boldsymbol{\varepsilon}(\mathbf{x}) = \mathbf{L}\mathbf{u}(\mathbf{x}) \tag{2}$$

in which

$$\mathbf{L} = \begin{bmatrix} \frac{\partial}{\partial x} & 0 & \frac{\partial}{\partial y} \\ \frac{\partial}{\partial y} & \frac{\partial}{\partial x} & 0 \end{bmatrix}^T \tag{3}$$

Substituting Eq. (1) into Eq. (2), we can get

$$\boldsymbol{\varepsilon}(\mathbf{x}) = \mathbf{B}(\mathbf{x})\mathbf{d} \tag{4}$$

where

$$\mathbf{B} = [\mathbf{B}_1, \mathbf{B}_2, \mathbf{B}_3] \tag{5}$$

$$\mathbf{B}_i = \begin{bmatrix} N_{i,x} & 0 & N_{i,y} \\ N_{i,y} & N_{i,x} & 0 \end{bmatrix}^T$$

In order to compensate the “over-stiffness” of the FEM model, a smoothed strain is introduced instead of compatible strain to “soften” the system. As shown in Fig. 1, the smoothed strain in the k th smoothing domain can be expressed as [5,6]

$$\bar{\boldsymbol{\varepsilon}}_k = \int_{\Omega_k} \boldsymbol{\varepsilon}(\mathbf{x}) \phi_k(\mathbf{x}) d\Omega \tag{6}$$

where $\phi_k(\mathbf{x})$ is a given smoothing function that satisfies at least unity property

$$\int_{\Omega} \phi_k(\mathbf{x}) d\Omega = 1 \quad (7)$$

A constant smoothing function is adopted as follows

$$\phi_k(\mathbf{x}) = \begin{cases} 1/A_k & \mathbf{x} \in \Omega_k \\ 0 & \mathbf{x} \notin \Omega_k \end{cases} \quad (8)$$

where A_k is the area of the smoothing domain Ω_k .

For interior edges, the smoothing domain Ω_k of edge k is formed by assembling two sub-domains Ω_{k1} and Ω_{k2} of two neighboring elements. The sub-domain Ω_{k1} and the sub-domain Ω_{k2} are from element $e1$ and element $e2$, respectively. The smoothed strain in smoothing domain Ω_k can be given by

$$\bar{\epsilon}_k = \frac{1}{A_k} \left(\int_{\Omega_{k1}} \epsilon_{k1}(\mathbf{x}) d\Omega + \int_{\Omega_{k2}} \epsilon_{k2}(\mathbf{x}) d\Omega \right) \quad (9)$$

where $\epsilon_{k1}(\mathbf{x})$ is the compatible strain calculated in element $e1$, and $\epsilon_{k2}(\mathbf{x})$ is the compatible strain calculated in element $e2$.

Since linear shape functions are used in the present method, the compatible strain is a constant in each smoothing sub-domain. Therefore, Eq. (9) can be rewritten as

$$\bar{\epsilon}_k = \frac{1}{A_k} (A_{k1} \epsilon_{k1} + A_{k2} \epsilon_{k2}) \quad (10)$$

where A_{k1} and A_{k2} are areas of the smoothing sub-domains Ω_{k1} and Ω_{k2} , respectively.

Substituting Eq. (4) into Eq. (10), the smoothed strain can be given by

$$\bar{\epsilon}_k = \frac{A_{k1}}{A_k} \mathbf{B}_{k1} \mathbf{d}_{k1} + \frac{A_{k2}}{A_k} \mathbf{B}_{k2} \mathbf{d}_{k2} = \bar{\mathbf{B}}_k \mathbf{d}_k \quad (11)$$

where \mathbf{d}_{k1} and \mathbf{d}_{k2} are the nodal displacements vector of the element $e1$ and the element $e2$, respectively, \mathbf{d}_k is the displacement vector of the nodes associated with edge k , \mathbf{B}_{k1} and \mathbf{B}_{k2} are the compatible strain matrices of the smoothing sub-domain Ω_{k1} and Ω_{k2} , respectively.

From Eq. (11), the smoothed strain matrix $\bar{\mathbf{B}}_k$ is written as

$$\bar{\mathbf{B}}_k = \frac{A_{k1}}{A_k} \mathbf{B}_{k1} + \frac{A_{k2}}{A_k} \mathbf{B}_{k2} \quad (12)$$

Note that the sign '+' denotes assembly but not sum here.

Using smoothed strain, the stress in the smoothing domain can be calculated by

$$\bar{\boldsymbol{\sigma}}_k = \mathbf{D}_{\text{eff}}^k \bar{\boldsymbol{\epsilon}}_k \quad (13)$$

In Eq. (13), $\mathbf{D}_{\text{eff}}^k$ is the effective material matrix for smoothing domain Ω_k , and is obtained from the effective constitutive equation, i.e.

$$\mathbf{D}_{\text{eff}}^k = \frac{E_{\text{eff}}^k}{1 - \nu_{\text{eff}}^k} \times \begin{bmatrix} 1 & \nu_{\text{eff}}^k & 0 \\ \nu_{\text{eff}}^k & 1 & 0 \\ 0 & 0 & (1 - (\nu_{\text{eff}}^k)^2)/2 \end{bmatrix} \text{ for plane stress} \quad (14)$$

where E_{eff}^k and ν_{eff}^k are effective Young's modulus and Poisson's ratio, which will be introduced in next section.

Using the smoothed strain obtained previously, we now seek for a weak form solution of displacement field \mathbf{u} that satisfies the following smoothed Galerkin weak form [6]

$$\int_{\Omega} \delta \bar{\boldsymbol{\epsilon}}^T \bar{\boldsymbol{\sigma}} d\Omega - \int_{\Omega} \delta \mathbf{u}^T \mathbf{b} d\Omega - \int_{\Gamma} \delta \mathbf{u}^T \mathbf{t} d\Gamma = 0 \quad (15)$$

where \mathbf{b} is the body force, and \mathbf{t} is the boundary traction.

Substituting Eqs. (1), (11) and (13) into Eq. (15), a set of discretized algebraic system equations can be obtained in the following matrix form

$$\bar{\mathbf{K}} \mathbf{d} - \mathbf{f} = 0 \quad (16)$$

where \mathbf{d} is the vector of nodal displacement at all the nodes, and \mathbf{f} is the force vector defined as

$$\mathbf{f} = \int_{\Omega} \mathbf{N}^T(\mathbf{x}) \mathbf{b} d\Omega + \int_{\Gamma} \mathbf{N}^T(\mathbf{x}) \mathbf{t} d\Gamma \quad (17)$$

In Eq. (16), $\bar{\mathbf{K}}$ is the (global) smoothed stiffness matrix of present ES-FEM, it is assembled in the form of

$$\bar{\mathbf{K}}_{ij} = \sum_{k=1}^{N_{\text{edge}}} \bar{\mathbf{K}}_{ij(k)} \quad (18)$$

The summation in Eq. (18) means an assembly process same as the practice in the FEM, N_{edge} is the number of the edges of the whole problem domain Ω , and $\bar{\mathbf{K}}_{ij(k)}$ is the stiffness matrix associated with Ω_k that is computed by

$$\bar{\mathbf{K}}_{ij(k)} = \int_{\Omega_k} (\bar{\mathbf{B}}_k)_i^T \mathbf{D}_{\text{eff}}^k (\bar{\mathbf{B}}_k)_j d\Omega = (\bar{\mathbf{B}}_k)_i^T \mathbf{D}_{\text{eff}}^k (\bar{\mathbf{B}}_k)_j A_k \quad (19)$$

3. Stress-strain relationship for effective material parameters

From the work of Jahed et al. [19], the strain-stress relationship can be taken in the form of

$$\epsilon_{ij} = f(\sigma_{ij}) \quad (20)$$

in which total strain ϵ_{ij} is the summation of an elastic part ϵ_{ij}^e and a plastic part ϵ_{ij}^p ,

$$\epsilon_{ij} = \epsilon_{ij}^e + \epsilon_{ij}^p \quad (21)$$

The elastic strain tensor relates to the stress tensor by Hooke's law for isotropic material

$$\epsilon_{ij}^e = \frac{1 + \nu}{E} \sigma_{ij} - \frac{\nu}{E} \sigma_{kk} \delta_{ij} \quad (22)$$

where ν is Poisson's ratio, E is Young's modulus, and δ_{ij} is the Delta function.

The plastic strain tensor is related to the deviatoric component of stress tensor and is given by Hencky's deformation theory

$$\epsilon_{ij}^p = \Phi S_{ij} \quad (23)$$

where

$$S_{ij} = \sigma_{ij} - \frac{1}{3} \sigma_{kk} \delta_{ij} \quad (24)$$

and Φ is a scalar valued function as given by

$$\Phi = \frac{3\epsilon_{\text{eq}}^p}{2\sigma_{\text{eq}}} = \frac{3}{2} \frac{\sqrt{2\epsilon_{ij}^p \epsilon_{ij}^p / 3}}{\sqrt{3S_{ij} S_{ij} / 2}} \quad (25)$$

Substituting Eqs. (22)–(25) into Eq. (21) yields

$$\varepsilon_{ij} = \left(\frac{1+\nu}{E} + \Phi \right) \sigma_{ij} - \left(\frac{\nu}{E} + \frac{1}{3}\Phi \right) \sigma_{kk} \delta_{ij} \quad (26)$$

All the variables inside the parentheses in Eq. (26) are involved with the material properties, final equivalent plastic strain and equivalent stress. This equation can be rewritten as

$$\varepsilon_{ij} = \left(\frac{1+\nu_{\text{eff}}}{E_{\text{eff}}} \right) \sigma_{ij} - \left(\frac{\nu_{\text{eff}}}{E_{\text{eff}}} \right) \sigma_{kk} \delta_{ij} \quad (27)$$

where E_{eff} and ν_{eff} are the equivalent Young's modulus and Poisson's ratio, which are given by

$$E_{\text{eff}} = \frac{1}{(1/E) + (2\Phi/3)} \quad (28)$$

$$\nu_{\text{eff}} = E_{\text{eff}} \left(\frac{\nu}{E} + \frac{\Phi}{3} \right) = E_{\text{eff}} \left(\frac{\nu}{E} + \frac{1}{2} \left(\frac{1}{E_{\text{eff}}} - \frac{1}{E} \right) \right) \quad (29)$$

4. Determination of effective material parameters

In the present section, projection method [25] is used for the determination of effective material parameters, E_{eff} and ν_{eff} , needed to calculate \mathbf{D}_{eff} . First, a linear elastic analysis is carried out to get the initial stress field. The equivalent stress using von Mises yield is used in comparison with the yield stress σ_0 . If the equivalent stress is smaller than the yield stress σ_0 , the computing is completed because the material is still in the elastic region; if the equivalent stress is larger than the yield stress σ_0 , it means that the deformation has already entered the plastic region, and the following iteration will be performed.

From the ES-FEM linear elastic analysis, we get the equivalent stress for each smoothing domain, and the state is shown as point 1 in Fig. 2. Keeping the strain value ε_1 the same (i.e. strain controlled), and projecting point 1 on the experimental uniaxial material curve to get point 1', the effective value of Young's modulus, $E_{\text{eff}}^{(1)}$, for the next iteration is obtained from the slope of the straight line 0–1'. Substituting this effective value into Eq. (29), the effective Poisson's

ratio, $\nu_{\text{eff}}^{(1)}$, can also be obtained. With the new effective material parameters the next ES-FEM linear elastic analysis is performed to get point 2 and its projection 2', and further to obtain $E_{\text{eff}}^{(2)}$ and $\nu_{\text{eff}}^{(2)}$. This iterative procedure is repeated until all the effective material parameters converge and equivalent stresses of all points fall on the experimental uniaxial stress–strain curve. The convergence is checked using following criterion

$$\sqrt{\frac{\sum_{k=1}^{N_{\text{edge}}} \left(E_{\text{eff}}^k(i+1) - E_{\text{eff}}^k(i) \right)^2}{\sum_{k=1}^{N_{\text{edge}}} \left(E_{\text{eff}}^k(i) \right)^2}} \leq \delta \quad (30)$$

where $E_{\text{eff}}^k(i)$ and $E_{\text{eff}}^k(i+1)$ are the effective Young's modulus of the i th and $(i+1)$ th iteration steps of the k th smoothing domain,

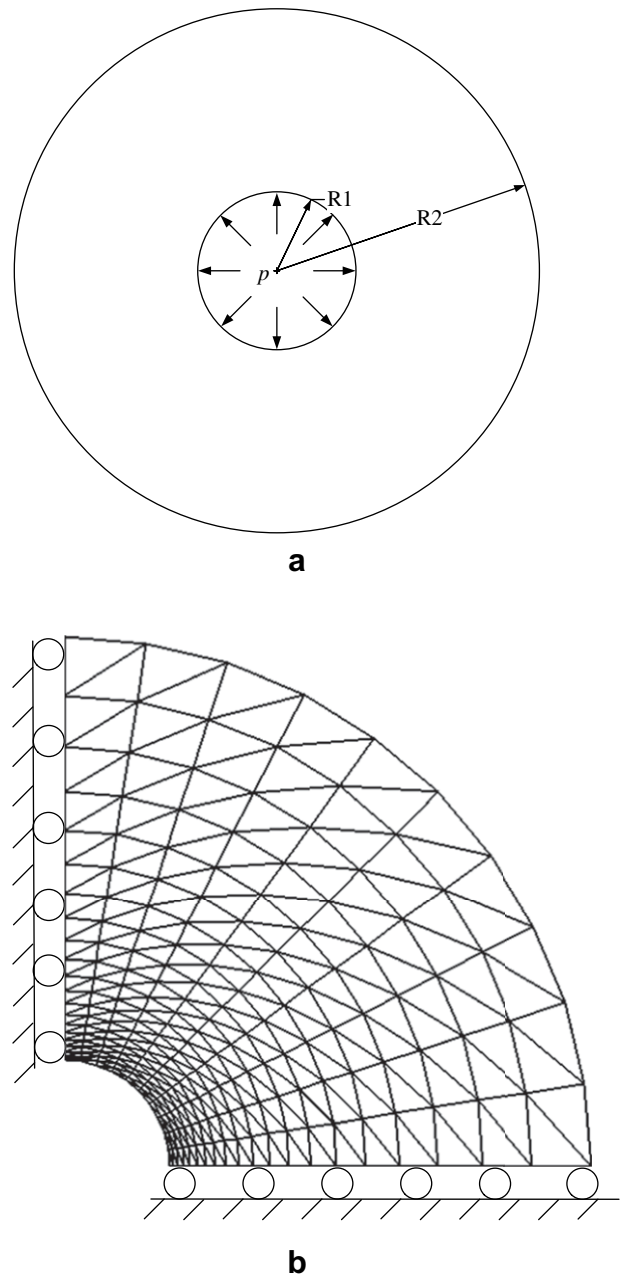


Fig. 3. Cylindrical pressure vessel subjected to internal pressure; (a) geometry and the boundary loading conditions; (b) mesh arrangement of the model.

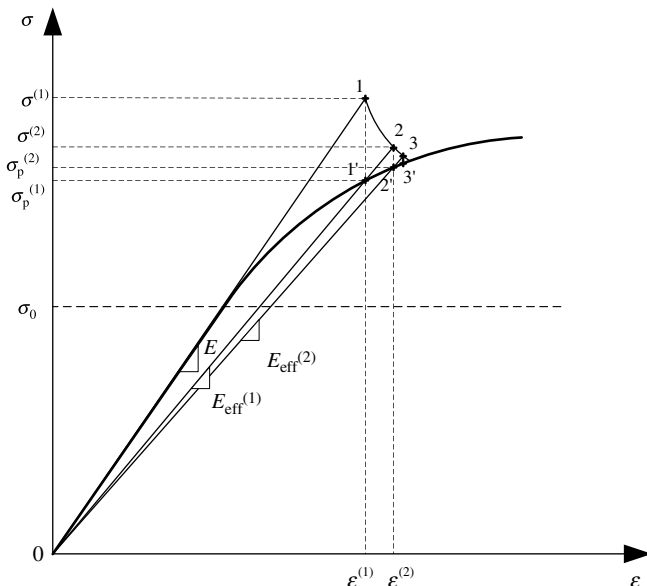


Fig. 2. Projection method for determination of E_{eff} .

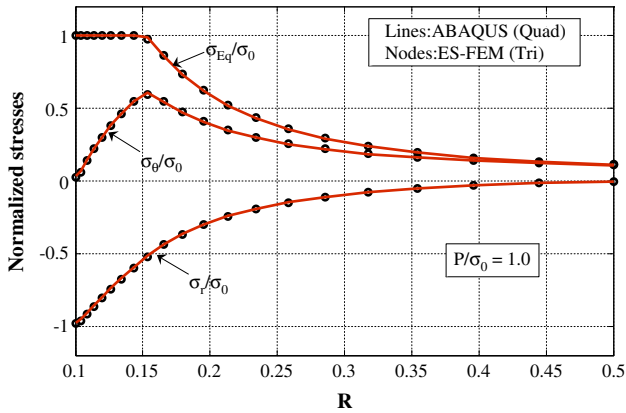


Fig. 4. Normalized stress distributions for elastic-perfectly plastic material. Lines: ABAQUS, nodes: ES-FEM.

respectively, and δ is the tolerance for convergence constant which is set to 10^{-3} in the study of the numerical examples.

It must be pointed out that if the applied loading is just large enough for the results failing to converge, the material is then regarded failed, and this loading is marked as the critical failure loading.

In this study, three different material models, elastic-perfectly plastic material, linearly work-hardening material and Ramberg–Osgood model, will be investigated for numerical examples. For elastic-perfectly plastic material, the stress–strain relation is given by

$$\varepsilon = \begin{cases} \sigma/E & \sigma < \sigma_0 \\ \sigma_0/E + \varepsilon^p & \sigma \geq \sigma_0 \end{cases} \quad (31)$$

Using Eq. (28), E_{eff} can be expressed by

$$E_{\text{eff}} = \frac{\sigma_0}{\varepsilon} \quad (32)$$

In the case of linearly work-hardening material model, it is assumed that the material has tangent modulus E_T . The material curve is

$$\varepsilon = \begin{cases} \sigma/E & \sigma < \sigma_0 \\ \sigma_0/E + (\sigma - \sigma_0)/E_T & \sigma \geq \sigma_0 \end{cases} \quad (33)$$

and E_{eff} is given by

$$E_{\text{eff}} = \frac{\sigma_0 + \varepsilon^p E_T}{\varepsilon} \quad (34)$$

Ramberg–Osgood model is one general case of hardening material, and is described by the following formulation

$$\frac{\varepsilon}{\varepsilon_0} = \frac{\sigma}{\sigma_0} + \alpha \left(\frac{\sigma}{\sigma_0} \right)^n \quad (35)$$

where $\varepsilon_0 = \sigma_0/E$ is the strain at initial yield, α is the yield offset, and n is the hardening exponent. Both α and n are preassigned material constants before computation. The effective Young's modulus E_{eff} is obtained as

$$E_{\text{eff}} = 1 / \left(\frac{1}{E} + \alpha \frac{\varepsilon_0}{\sigma_0} \left(\frac{\sigma}{\sigma_0} \right)^{n-1} \right) \quad (36)$$

For a determined strain, the stress state according to the strain can be calculated from Eq. (35) using a nonlinear equation solver. E_{eff} can then be evaluated from Eq. (36). Once E_{eff} is determined, ν_{eff} can be obtained from Eq. (29).

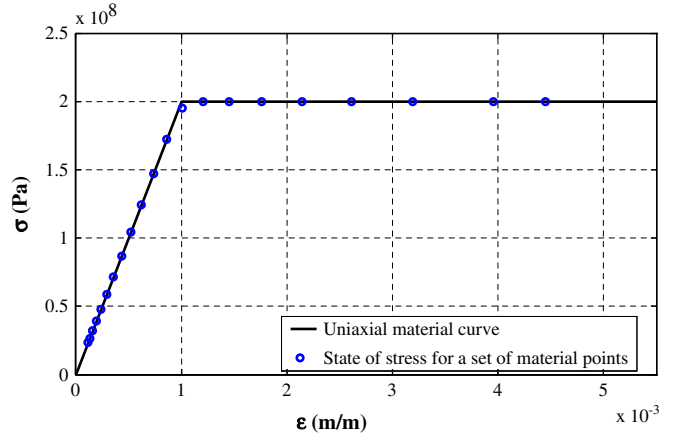


Fig. 5. State of stress for a set of nodes in radial direction after convergence for elastic-perfectly plastic material.

5. Numerical examples

5.1. Cylindrical vessel

To illustrate the validity of the proposed ES-FEM in material nonlinear problems, a cylindrical vessel under plane stress conditions subjected to an internal loading pressure P is investigated. The geometry and the boundary conditions are shown in Fig. 3a. The inner radius is $R1 = 0.1$ m, and the outer radius is $R2 = 0.5$ m. The material properties are taken as Young's modulus $E = 2.0 \times 10^{11}$ Pa, Poisson ratio $\nu = 0.3$, and yield stress $\sigma_0 = 2.0 \times 10^8$ Pa. For linearly work hardening case, the tangent modulus is taken as $E_T = E/4$. For Ramberg–Osgood model, the yield offset $\alpha = 3/7$ and hardening exponent $n = 5$ are considered. Owing to the symmetry conditions, only a quarter of the cylindrical vessel is modeled, and the model is divided into 20×10 elements, as shown in Fig. 3b.

To validate the accuracy of the present solutions, the analysis using the finite element commercial software ABAQUS is also carried out using quadrilateral element with the same discretization nodes. At first, the material is considered as elastic-perfectly plastic model. The variations of radial, hoop and equivalent von Mises stresses along the thickness direction of the cylinder for pressure ratio $P/\sigma_0 = 1.0$ are shown in Fig. 4. In present ES-FEM, the stress values at node are obtained by averaging the values of the

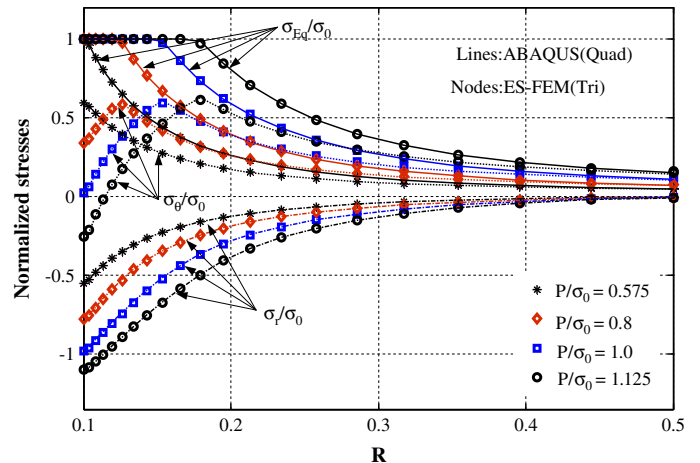


Fig. 6. Normalized stress distribution for different pressure ratios for elastic-perfectly plastic material. Lines: ABAQUS, nodes: ES-FEM.

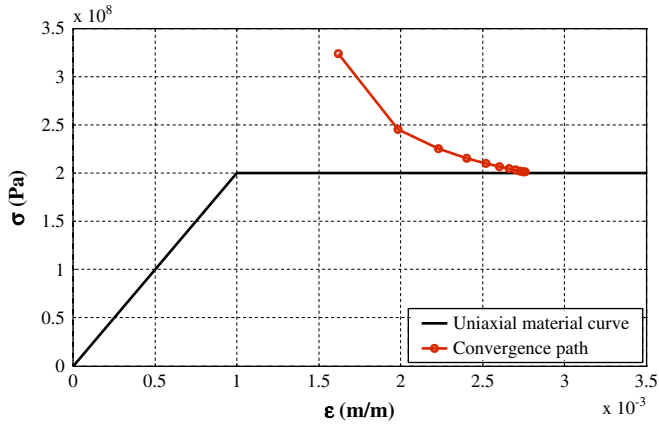


Fig. 7. The convergence path for a particular point for elastic-perfectly plastic material.

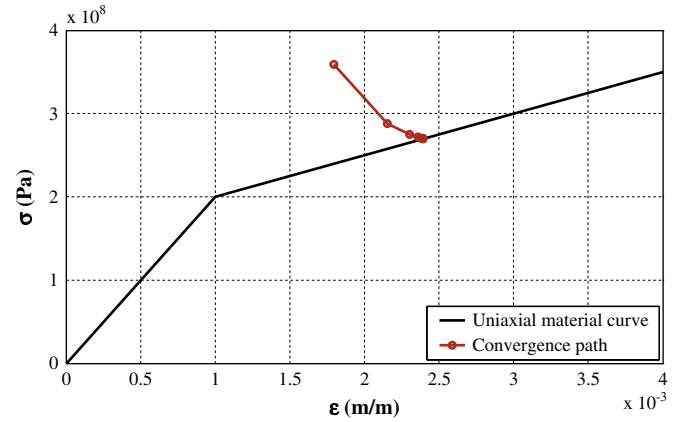


Fig. 10. The convergence path for a particular point for linearly hardening material model.

associated smoothing domains. It is observed that the present stresses' nodes consist well with ABAQUS curve all along. Fig. 5 demonstrates the state of von Mises stress for a set of nodes in radial direction after convergence. It can be seen that all the nodes are in good agreement with the uniaxial material curve. Fig. 6 gives the stress variations for different internal pressure ratios. The dimension of the plastic zone can be easily estimated from stress distributions, which compares well with ABAQUS quadrilateral

element. As elastic-perfectly plastic model is used, the von Mises stresses in plastic zone are all equal to yield stress σ_0 .

Fig. 7 shows the convergence path for a material point during the process of iteration. Here, convergence is assumed to be achieved when Eq. (30) is satisfied. It can be seen that the point falls on the uniaxial material curve quickly. Fig. 8 presents the load–displacement

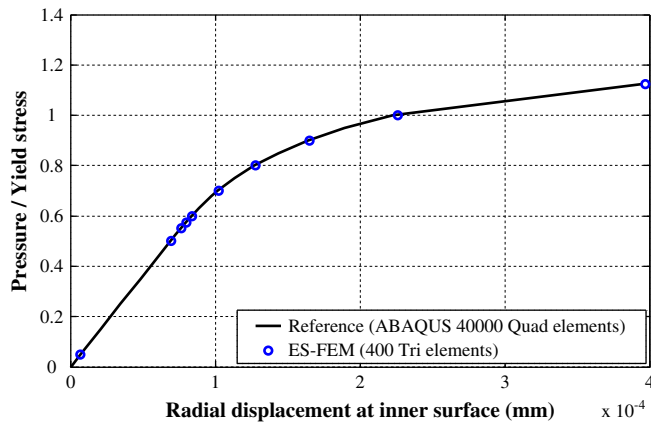


Fig. 8. The radial displacement at inner surface with different pressure using elastic-perfectly plastic material.

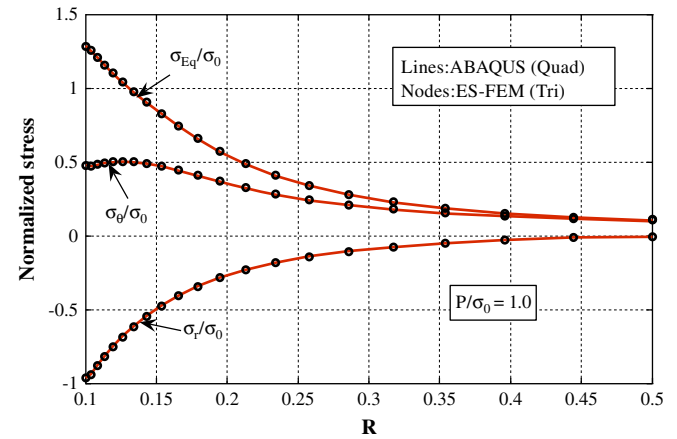


Fig. 11. Normalized stress distributions for Ramberg–Osgood material model. Lines: ABAQUS, nodes: ES-FEM.

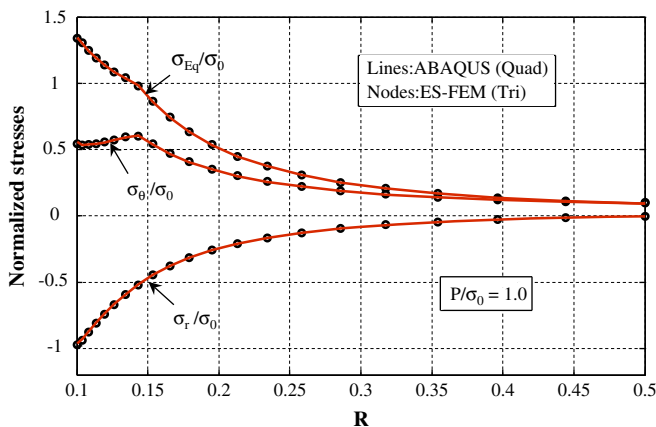


Fig. 9. Normalized stress distributions for linearly hardening material model. Lines: ABAQUS, nodes: ES-FEM.

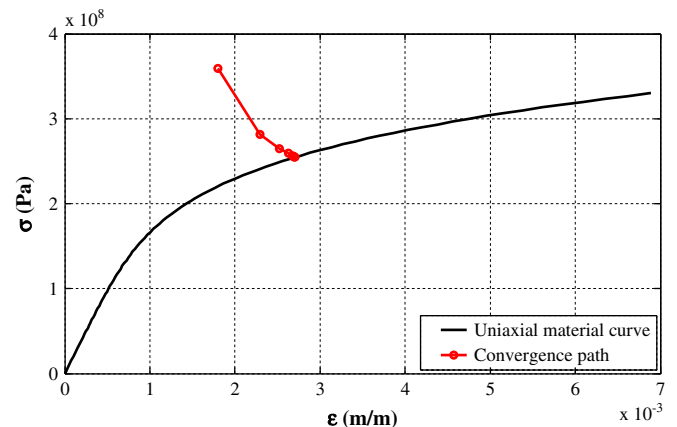


Fig. 12. The convergence path for a particular point for Ramberg–Osgood material model.

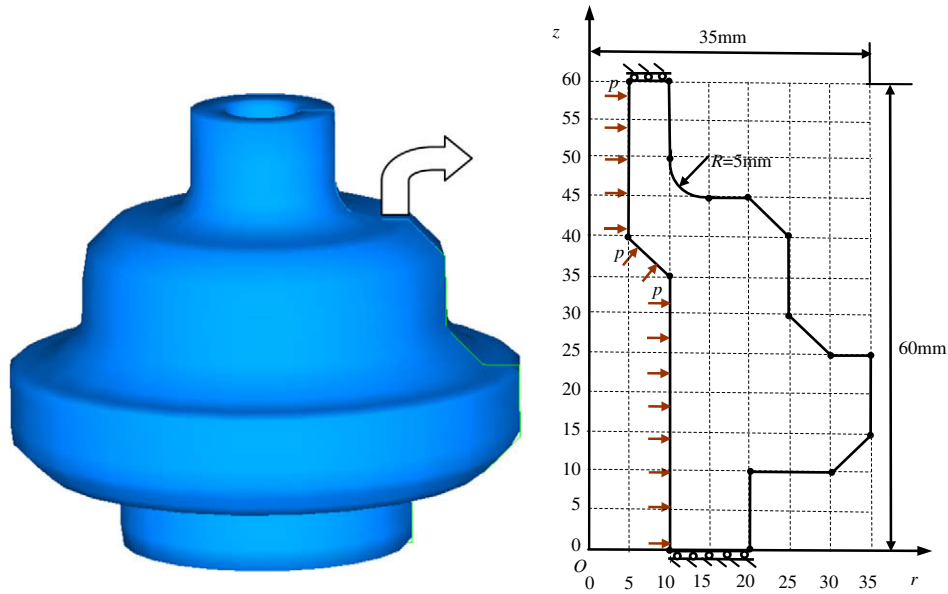


Fig. 13. A nozzle subjected to internal pressure, geometry and the boundary loading conditions.

curves obtained by the present method. For comparison, the reference solutions obtained using ABAQUS with large number of quadrilateral elements (40,000) are also plotted in the same figure. It is obvious that the ES-FEM method gives very accurate results.

The example is performed again using the linearly hardening material model. The distributions of the von Mises stress, hoop stress and radial stress are all shown in Fig. 9. It clearly shows that the solutions using present ES-FEM coincide well with those of ABAQUS quadrilateral element. We can easily find that plastic deformation occurs in the region in which the normalized equivalent von Mises stress is larger than 1.0. Because of the material work hardening, the normalized equivalent von Mises stress in the plastic region no longer remains at 1.0. Fig. 10 shows the convergence path for a particular point using linearly hardening

material model. It can be observed that all the nodes fall on the uniaxial material curve quickly.

A Ramberg–Osgood material model with yield offset $\alpha = 3/7$ and hardening exponent $n = 5$ is also considered for this problem. The results are shown in Figs. 11 and 12. It is observed again that the present solutions match well with those of ABAQUS quadrilateral element and the final stress–strain state as well as the convergence path are quite reasonable.

5.2. A nozzle with internal pressure

A nozzle subjected to internal pressure is analyzed to demonstrate more features of the present method. The geometry and the numerical model are shown in Fig. 13. The same case is also

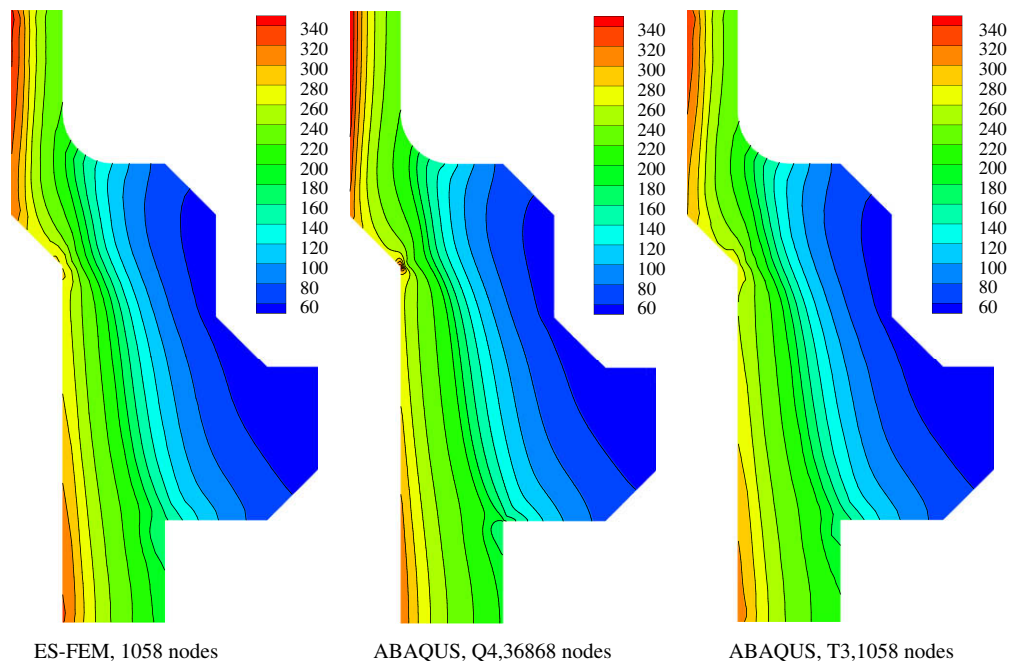


Fig. 14. Comparison of computed von Mises stress distributions.

analyzed using ABAQUS with triangular element and a reference solution is also computed using ABAQUS quadrilateral elements with large number of nodes (36,868) for comparison. Linear work-hardening material model is employed here, and the material parameters are given as Young's modulus $E = 2.1 \times 10^5$ MPa, Poisson ratio $\nu = 0.3$, yield stress $\sigma_0 = 210$ MPa, and the tangent modulus is taken as $E_T = E/4$. The internal pressure p is equal to the yield stress σ_0 .

Fig. 14 shows the comparison of computed von Mises stress distributions between the present method, ABAQUS using the same triangular elements and the reference ones obtained using ABAQUS with fine mesh (36,868) of quadrilateral elements. It is clearly shown that the present result agrees better with reference solution than those obtained using ABAQUS triangular elements with the same mesh, especially in the zone of large von Mises.

6. Conclusions

In this paper, the edge-based smoothed finite element method (ES-FEM) is formulated to analyze material nonlinear problems. In present ES-FEM, the smoothed Galerkin weak form is used for discretizing the system equations and the numerical integration is performed based on the smoothing domains associated with edges of the mesh. Material nonlinearity is considered as pseudo-linear elastic analysis by suitable updating of material properties in terms of effective material parameters. Based on Hencky's total deformation theory, the effective elastic material parameters can be easily obtained in an iterative procedure from the one-dimensional uniaxial material curve. Numerical examples using von Mises material have been successfully analyzed obeying elastic-perfectly plastic, linearly work-hardening or Ramberg–Osgood hardening model, respectively, and very good results have been obtained. Through these investigations, the following conclusions can be drawn.

- (1) In the present ES-FEM, the formulation is straightforward and the implementation is as easy as the FEM, without the increase of degree of freedoms. Hence the present method is very simple and can be easily implemented with little changes to the FEM code.
- (2) Through smoothing operation, the present method can provide a much needed softening effect to the model and the "overly-stiff" phenomenon of the compatible displacement-based FEM model is ameliorated effectively. Therefore, the performance of the present method is greatly enhanced, and numerical results obtained using triangular elements achieve the same accuracy level as ABAQUS quadrilateral elements.
- (3) In the proposed method, many techniques used in linear elastic analysis can be easily incorporated here with only minor revisions. Compared with the conventional inelastic analysis using classical incremental theory and Newton–Raphson method, the present scheme can be easily implemented in a numerically straightforward way.

Acknowledgements

The support of National Outstanding Youth Foundation (50625519), Key Project of National Science Foundation of China (60635020), Program for Changjiang Scholar and Innovative Research Team in University and the China-funded Postgraduates' Studying Abroad Program for Building Top University are gratefully acknowledged. The authors also give sincerely thanks to the support of Centre for ACES, Singapore-MIT Alliance (SMA), and National University of Singapore.

References

- [1] Belytschko T, Liu WK, Moran B. Nonlinear finite elements for continua and structures. Chichester, England: John Wiley & Sons; 2000.
- [2] Kojic M, Bathe KJ. Inelastic analysis of solids and structures. Berlin: Springer-Verlag; 2005.
- [3] Crisfield MA. Non-linear finite element analysis of solids and structures. Chichester, England: John Wiley & Sons; 1997.
- [4] Owen DRJ, Hinton E. Finite element in plasticity: theory and practice. Swansea, U.K.: Pineridge Press Limited; 1980.
- [5] Chen JS, Wu CT, Yoon S, You Y. A stabilized conforming nodal integration for Galerkin meshfree methods. International Journal for Numerical Methods in Engineering 2001;50:435–66.
- [6] Liu GR. A generalized gradient smoothing technique and smoothed bilinear form for Galerkin formulation of a wide class of computational methods. International Journal of Computational Methods 2008;5(2):199–236.
- [7] Liu GR. A G space theory and weakened weak (W2) form for a unified formulation of compatible and incompatible methods: part I theory and part II application to solid mechanics problems. International Journal for Numerical Methods in Engineering, in press.
- [8] Liu GR, Dai KY, Nguyen TT. A smoothed finite element method for mechanics problems. Computational Mechanics 2007;39:859–77.
- [9] Liu GR, Nguyen TT, Dai KY, Lam KY. Theoretical aspects of the smoothed finite element method (SFEM). International Journal for Numerical Methods in Engineering 2007;71:902–30.
- [10] Cui XY, Liu GR, Li GY, Zhao X, Nguyen TT, Sun GY. A smoothed finite element method (SFEM) for linear and geometrically nonlinear analysis of plates and shells. CMES Computer Modeling in Engineering & Sciences 2008;28(2):109–26.
- [11] Liu GR, Nguyen TT, Nguyen-Xuan H, Lam KY. A node-based smoothed finite element method (NS-FEM) for upper bound solutions to solid mechanics problems. Computer & Structures 2009;87:14–26.
- [12] Liu GR, Zhang GY, Dai KY, Wang YY, Zhong ZH, Li GY, et al. A linearly conforming point interpolation method (LC-PIM) for 2D solid mechanics problems. International Journal of Computational Methods 2005;2:645–65.
- [13] Liu GR, Zhang GY. Upper bound solution to elasticity problems: a unique property of the linearly conforming point interpolation method (LC-PIM). International Journal for Numerical Methods in Engineering 2008;74:1128–61.
- [14] Wu SC, Liu GR, Zhang HO, Zhang GY. A node-smoothed point interpolation method (NS-PIM) for three-dimensional thermoelastic problems. Numerical Heat Transfer, Part A: Applications 2008;54:1121–47.
- [15] Liu GR, Nguyen TT, Lam KY. An edge-based smoothed finite element method (ES-FEM) for static, free and forced vibration analysis. Journal of Sound and Vibration 2008. doi:10.1016/j.jsv.2008.08.027.
- [16] Neuber H. Theory of stress concentration for shear-strained prismatical bodies with arbitrary non-linear stress-strain law. Journal of Applied Mechanics ASME 1961;28(4):550–4.
- [17] Dhalla AK, Jones GL. ASME code classification of pipe stresses: a simplified procedure. International Journal of Pressure Vessels and Piping 1986;26:145–66.
- [18] Seshadri R. The generalized local stress strain (GLOSS) analysis—theory and applications. Journal of Pressure Vessel Technology Transactions of the ASME 1991;113:219–27.
- [19] Jahed H, Sethuraman R, Dubey RN. A variable material property approach for solving elastic-plastic problems. International Journal of Pressure Vessels and Piping 1997;71:285–91.
- [20] Babu S, Iyer PK. Inelastic analysis of components using a modulus adjustment scheme. Journal of Pressure Vessel Technology Transactions of the ASME 1998;120:1–5.
- [21] Chen HF, Ponter ARS. Shakedown and limit analyses for 3-D structures using the linear matching method. International Journal of Pressure Vessels and Piping 2001;78:443–51.
- [22] Chen HF, Ponter ARS. Shakedown and limit analyses for 3-D structures using the linear matching method. International Journal of Pressure Vessels and Piping 2004;81:327–36.
- [23] Chen HF, Ponter ARS, Ainsworth RA. The linear matching method applied to the high temperature life integrity of structures. Part 1. Assessments involving constant residual stress fields. International Journal of Pressure Vessels and Piping 2006;83:123–35.
- [24] Chen HF, Ponter ARS, Ainsworth RA. The linear matching method applied to the high temperature life integrity of structures. Part 2. Assessments beyond shakedown involving changing residual stress fields. International Journal of Pressure Vessels and Piping 2006;83:136–47.
- [25] Desikan V, Sethuraman R. Analysis of material nonlinear problems using pseudo-elastic finite element method. Journal of Pressure Vessel Technology Transactions of the ASME 2000;122:457–61.
- [26] Sethuraman R, Reddy CS. Pseudo elastic analysis of material nonlinear problems using element free Galerkin method. Journal of the Chinese Institute of Engineers 2004;27(4):505–16.
- [27] Dai KY, Liu GR, Han X, Li Y. Inelastic analysis of 2D solids using a weak-form RPIM based on deformation theory. Computer Methods in Applied Mechanics and Engineering 2006;195:4179–93.
- [28] Gu YT, Wang QX, Lam KY, Dai KY. A pseudo-elastic local meshless method for analysis of material nonlinear problems in solids. Engineering Analysis with Boundary Elements 2007;31:771–82.